J. Membrane Biol. 164, 125–138 (1998)

The Journal of
Membrane
Biology

Characteristics of Single, Large-Conductance Calcium-Dependent Potassium Channels (BK_{Ca}) from Smooth Muscle Cells Isolated from the Rabbit Mesenteric Artery

D.K. Mistry, C.J. Garland

Department of Pharmacology, School of Medical Sciences, University of Bristol, University Walk, Bristol BS8 1TD, United Kingdom

Received: 22 December 1997/Revised: 27 March 1998

Abstract. Smooth muscle cells isolated from the secondary and tertiary branches of the rabbit mesenteric artery contain large Ca^{2+}-dependent channels. In excised patches with symmetrical (140 mM) K^+ solutions, these channels had an average slope conductance of 235 ± 3 pS, and reversed in direction at −6.1 ± 0.4 mV. The channel showed K^+ selectivity and its open probability (P_o) was voltage-dependent. Iberiotoxin (50 nM) reversibly decreased P_o, whereas tetraethylammonium (TEA, at 1 mM) reduced the unitary current amplitude. Apamin (200 nM) had no effect. The channel displayed sublevels around 1/3 and 1/2 of the mainstate level. The effect of $[Ca^{2+}]$ on P_o was studied and data fitted to Boltzmann relationships. In 0.1, 0.3, 1.0 and 10 μM Ca^{2+}, $V_{1/2}$ was 77.1 ± 5.3 ($n = 18$), 71.2 ± 4.8 ($n = 16$), 47.3 ± 10.1 ($n = 11$) and −14.9 ± 10.1 mV ($n = 6$), respectively. Values of k obtained in 1 and 10 μM $[Ca^{2+}]$ were significantly larger than that observed in 0.1 μM $[Ca^{2+}]$. With 30 μM NS 1619 (a BK_{Ca} channel activator), $V_{1/2}$ values were shifted by 39 mV to the left (hyperpolarizing direction) and k values were not affected. TEA applied intracellularly, reduced the unitary current amplitude with a K_d of 59 mM. In summary, BK_{Ca} channels show a particularly weak sensitivity to intracellular TEA and they also display large variation in $V_{1/2}$ and k. These findings suggest the possibility that different types (isoforms) of BK_{Ca} channels may exist in this vascular tissue.

Key words: Rabbit mesenteric artery — TEA — Ca^{2+}-dependent K^+ channel-BK_{Ca} — NS 1619

Introduction

Large conductance K^+ channels that are activated by intracellular Ca^{2+} and membrane depolarization have been found in virtually every type of smooth muscle. These have now been called BK_{Ca} to distinguish them from a smaller conductance Ca^{2+} dependent K^+ channels (SK_{Ca}) which are inhibited by the bee venom peptide apamin in vascular tissue (Marchenko & Sage, 1996; Vogalis & Goyal, 1997). Properties of BK_{Ca} channels include block by external TEA ($K_d = 200$ μM), block by the scorpion toxins charybdotoxin and iberiotoxin ($K_d < 10$ nM in both cases). BK_{Ca} are not inhibited by low concentrations of extracellular barium (100 μM) which inhibit both ATP-dependent K^+ channel (K_{ATP}) and inward rectifier K^+ channels, K_{IR} (Nelson & Quayle, 1995).

Inspite of their ubiquitous occurrence, their role in vascular smooth muscle has remained elusive. In general, hyperpolarization in this tissue appears to be associated with vasodilatation, and depolarization appears to be associated with vasoconstriction (Nelson & Quayle, 1995). The activation of BK_{Ca} would be expected to be associated with vasodilatation under conditions in which intracellular calcium is raised. Increase in internal pressure causes an elevation of free intracellular calcium in resistance arteries, thereby increasing the tone of smooth muscle cells, a phenomenon known as 'myogenic tone.' It has been suggested that one of the functions of BK_{Ca} channels is to limit myogenic tone and thereby prevent damage to the tissues during near maximum constriction of arterioles (Brayden & Nelson, 1992). Blockers of BK_{Ca} depolarize and constrict arteries with tone. Thus, tetraethylammonium (TEA), charybdotoxin and iberiotoxin depolarized and constricted myogenic cerebral and coronary arteries. These observations suggest that BK_{Ca} channels play a dynamic role in the control of arterial smooth muscle membrane potential by serving as a negative feedback pathway to regulate the degree of membrane depolarization and hence vasoconstriction caused by pressure and other vasoconstrictors (Nelson & Quayle, 1995). Other proposed roles for Ca^{2+}-activated K^+ channels in arterial smooth muscle include repolar-

Correspondence to: C.J. Garland

ization of action potential and regulation of resting membrane potential (Treischmann & Isenberg, 1989; Brayden & Nelson, 1992; Asano et al., 1993). Vasorelaxants such as nitric oxide (NO) can also modulate BK_{Ca} channels in smooth muscle by both direct (Bolotina et al., 1994) and indirect mechanisms (George & Shibata, 1995).

It is clear from the above observations that BK_{Ca} channels play an important role in the functioning of vascular smooth muscle. A description of single BK_{Ca} channels from rabbit mesenteric arteries has previously not been available, hence we have used the patch-clamp technique to study the single-channel properties of this channel. Some of these results have been presented in a preliminary form (Mistry & Garland, 1996).

Materials and Methods

Female white rabbits (1.8–2.5 kg) were anesthetized with sodium pentobarbitone (60 mg/kg i.v.) and killed by rapid exsanguination. A segment of lower ileum plus attached mesentery was removed from the animal. Mesenteric arteries of the secondary and tertiary branches were cleaned of connective tissue and cut open longitudinally into 1–2 mm strips. The strips of arteries were stored at 4°C for 1 hr. The tissue was then placed in a 0 Ca^{2+} solution for 15 min at 37°C, and then transferred to an enzyme mixture at 37°C containing 1 mg/ml collagenase, 2 mg/ml bovine serum albumin and 0.70 mg/ml pronase (all from Sigma) for 45 mins. The enzyme mixture had a volume of 3 ml and contained a [Ca^{2+}] of 15 μM. The tissue was then shaken intermittently during this period and then transferred to a 0 Ca^{2+} solution which was enzyme free, and gently triturated with a 1-mm and then a 0.5-mm Pasteur pipette until the suspension became cloudy. The resulting cell suspension was stored at 4°C and used within 9 hr of isolation. A drop of the cell suspension was placed in the center of a 35-mm tissue culture dish (Nunc) and mounted on an inverted microscope (Nikon 200 UK).

The external (Tyrode) solution contained (in mM): 130 NaCl, 5 KCl, 1.2 $MgCl_2$, 10 HEPES, 10 glucose, 1.2 $CaCl_2$, pH 7.3 (buffered with NaOH). The pipette solution contained (in mM); 130 KCl, 2 Na_2ATP, 3 $MgCl_2$, 10 HEPES, 1 EGTA, pH 7.3 (buffered with KOH). The above two solutions were used for outside-out patch experiments. For the inside-out patches, the pipette (extracellular) solution contained (in mM): 140 KCl, 10 HEPES, 1 $CaCl_2$, 1 $MgCl_2$, pH 7.3 (buffered with KOH). Iberiotoxin (IBTX), apamin and tetraethylammonium (TEA) were purchased from Sigma and NS 1619 was obtained from RBI. The intracellular solutions containing 0.1, 0.3, 1.0 and 10 μM free Ca^{2+} were made up from different combinations of EGTA and $CaCl_2$ as used previously to study large conductance Ca^{2+}-activated K^+ channels in rat pulmonary artery smooth muscle cells (Albarwani et al., 1994). In more detail, the 0.1 μM Ca^{2+} solution contained 5.12 mM $CaCl_2$ and 7 mM EGTA, the 0.3 μM Ca^{2+} solution contained 5.35 mM $CaCl_2$ and 6 mM EGTA, the 1.0 μM Ca^{2+} solution, contained 4.81 mM $CaCl_2$ and 5 mM EGTA and the 10.0 μM solution contained 3.0 mM $CaCl_2$ and 3 mM EGTA. This was in addition to 140 mM KCl and 1 mM $MgCl_2$, the concentration of free Ca^{2+} was determined using a program for calculating metal ion to ligand binding (Peter Griffiths, University Laboratory of Physiology, Oxford).

Excised patches were obtained using the patch-clamp technique at 20–25°C (Hamill et al., 1981). Patch pipettes were made from borosilicate glass (Clarke, Electromedical Instruments o.d. 1.5 mm, i.d. 0.86 mm) and had resistances of 4–10 MΩ after fire polishing. The patch-clamp amplifier was an axopatch 1D (Axon Instruments, Foster City, CA) and data were stored on a 486 PC after digitization by a digidata 1200 interface (Axon Instruments).

Voltage-clamp command paradigms and data analysis were performed using Pclamp 6.20 software (Axon Instruments) and FigP (Biosoft, Cambridge UK). Unitary current amplitude was determined from amplitude histograms fitted with Gaussian functions. Sublevel amplitude was also determined from amplitude histograms and only sublevels lasting > 0.3 msec were included in the analysis. Opening probability (P_o) was determined from the following relation:

$$P_o = \sum_{i=1}^{N} t_i i/(TN)$$

where t_i is the time spent with $i = 1, 2, \ldots N$ channels open and where N is the number of channels, i = unitary current and T is the sample length (60 sec). The maximum number of open conductance levels (N) was observed under conditions of high P_o (i.e., at large positive potentials and high [Ca^{2+}]). Other equations used in this study include the Hill equation to assess the action of intracellular TEA on BK_{Ca}

$$I_{\text{Norm}} = 1/1 + ([TEA^+]/K_d)^H$$

where H is the Hill Coefficient and K_d is the dissociation Constant and I_{Norm} is the normalized current = $I_{TEA}/I_{\text{CONTROL}}$

The Boltzmann relation was also used to assess the effect of voltage on opening probability (P_o)

$$P_o/P_{\max} = (1 + \exp((V - V_{1/2})/k))^{-1}$$

where $V_{1/2}$ is the voltage at which $P_o = 0.5$ and k is the steepness factor (voltage required to produce an e fold change in P_o).

The pipette solutions were frozen in aliquots at −18°C and defrosted and filtered prior to use (pore size 0.2 μm, Gelman sciences). Liquid junction potentials between the pipette and bath solutions were measured using a 3M KCl reference electrode and found to be ≤4 mV, hence corrections for these potentials were not made. Drugs were applied using a local perfusion pipette which had a diameter of approximately 200 μm. The perfusion pipette was positioned approximately 200–400 μm from the patch under study. Leakage current was determined by measuring the mean inward current when the patch was hyperpolarized from the holding potential. Single-channel currents were filtered at 5 kHz (−3 dB) and digitized at 10 kHz. Results are expressed as mean ± SE mean unless otherwise stated. The open probability of BK_{Ca} proved to be quite variable from patch to patch, even from patches obtained from the same cell, hence the paired t-test was used to assess the action of drugs. A P value < 0.05 was considered significant. Statistical comparisons were also made using the ANOVA test.

Results

Inside-Out Patches

Virtually all inside-out patches contained large unitary currents that increased in activity with patch depolarization and in the symmetrical (140 mM) K^+ solutions employed, reversed in direction close to 0 mV. As described earlier, properties of BK_{Ca} channels include activation by intracellular Ca^{2+}. With a [Ca^{2+}] of 0.1 μM, channel openings were primarily evident at positive patch potentials, and openings at negative patch poten-

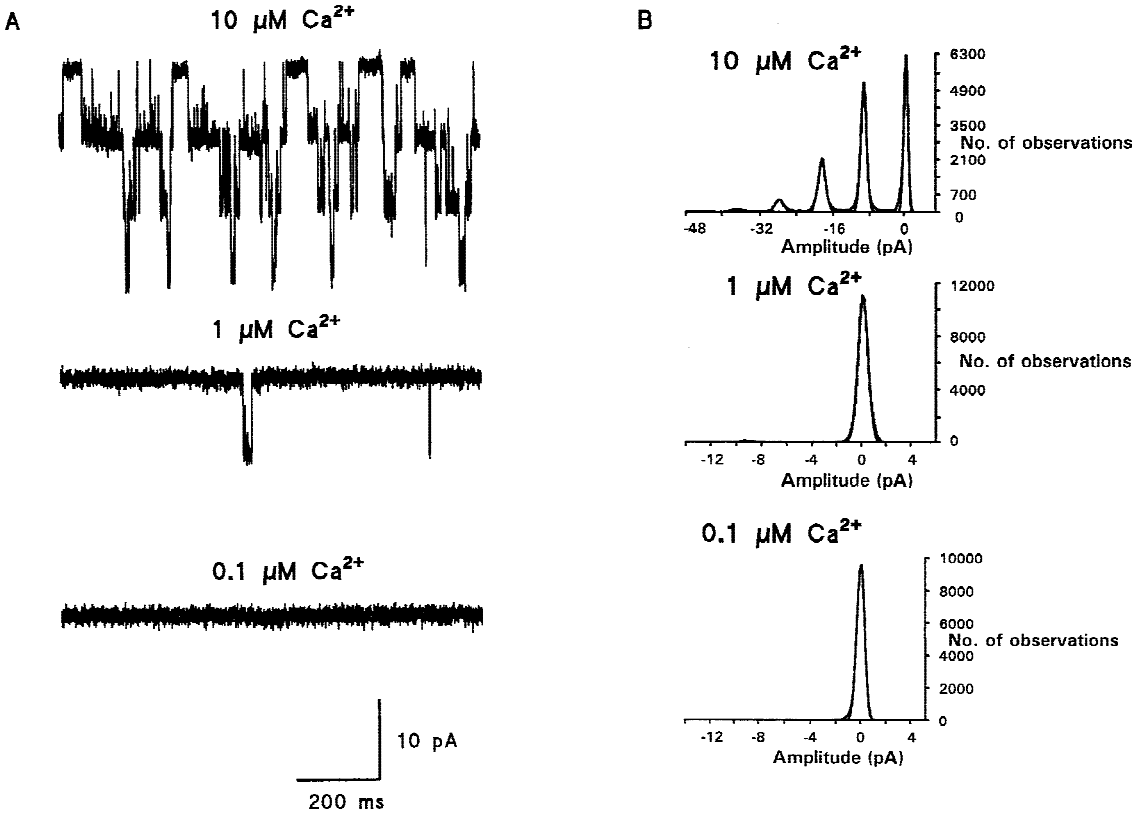

Fig. 1. Activation of K^+ channels by 1 and 10 μM Ca^{2+} in inside-out patches from freshly isolated smooth muscle cells of the mesenteric artery. (*A*) Increasing [Ca^{2+}] from 0.1 to 1 and 10 μM in an inside-out patch. In the presence of 0.1 μM Ca^{2+} the patch was quiet, while the application of 1 μM Ca^{2+} activated one large inward ion channel. Switching to a solution containing 10 μM Ca^{2+} activated a further three channels. With both 1 and 10 μM [Ca^{2+}] the activation was fully reversible. The patch potential was −40 mV. (*B*) Amplitude histograms in the three different concentrations of Ca^{2+}. The amplitude histogram with 10 μM Ca^{2+} was fitted by the sum of five Gaussians with peaks at 0, 9.21, 18.27, 27.47, and 37.5 pA. The amplitude histogram in 1.0 μM Ca^{2+} was fitted by the sum of two Gaussians with peaks at 0 and 9.26 pA, while the amplitude histogram in 0.1 μM Ca^{2+} was fitted by a single Gaussian which had a peak at 0 pA.

tials were either infrequent or absent. At positive patch potentials, application of either 1 or 10 μM Ca^{2+} to the inside face of the patch produced a large increase in channel activity, with up to 10 channels being recorded at one time. As a result of this increased activity of patches at positive potentials, individual channels activated by Ca^{2+} (1 or 10 μM) could not be resolved. Hence, Ca^{2+} was applied at negative patch potentials where there was little, if any channel activity. Under these conditions, either 1 or 10 μM Ca^{2+} activated inward channels whose amplitude increased with patch hyperpolarization. Figure 1*A* shows examples of an inside-out patch in 10, 1 and 0.1 μM Ca^{2+} at a patch potential of −40 mV. In the presence of 0.1 μM Ca^{2+}, no channel openings were observed, but large inward currents were activated in both 1 and 10 μM Ca^{2+}. The total amplitude histograms in the three different [Ca^{2+}] are shown in Fig. 1*B*.

Raising [Ca^{2+}] had no effect on unitary current amplitude of the channel but greatly increased the number of channels activated and their activity. In symmetrical (140 mM) K^+ solutions, and between ±70 mV, the slope conductance of these unitary currents was linear. The average slope conductance was 235 ± 3 pS ($n = 24$) and the mean reversal potential was −6.1 ± 0.4 mV in 1 or 10 μM Ca^{2+}. The data points in symmetrical KCl solutions were fitted by linear regression, and a permeability value (P_K) of 4.55×10^{-13} $cm^3 sec^{-1}$ was calculated from the relation

$$I_K = P_K(VF^2[K^+])/(RT)$$

where V is the patch potential, F is the Faraday constant, R is the gas constant and T is the absolute temperature. To assess the K^+ selectivity of the channel, the high [K^+] was replaced by Tyrode solution containing 5 mM K^+ and the [Ca^{2+}] was reduced to approximately 1 μM. Under these conditions, the *i-v* relationship showed rectification and the reversal potential shifted in a manner predicted by the Nernst relationship for K^+. Under the conditions employed the exact reversal potential was not observed owing to the poor single-to-noise ratio and the large

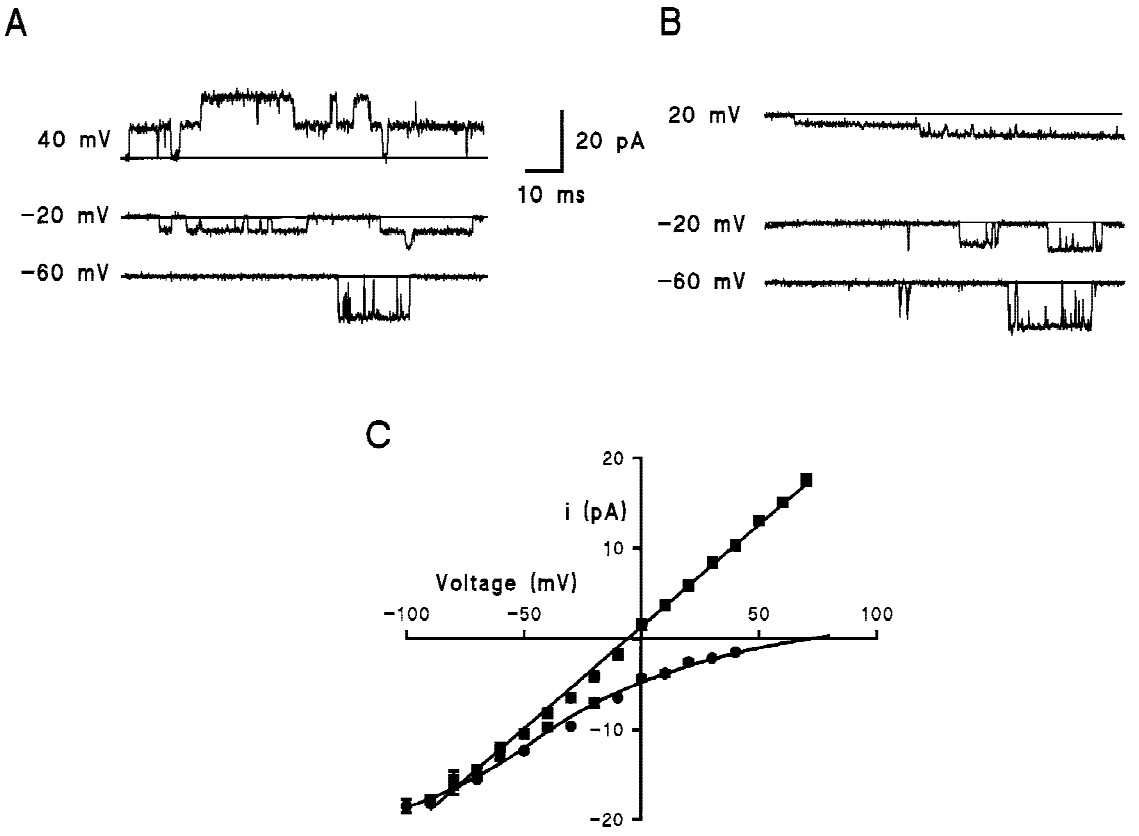

Fig. 2. Examples of large unitary currents recorded in inside-out patches from rabbit mesenteric arteries. (*A*) Records of unitary currents in the presence of 1 μM Ca^{2+} at 40, −20 and −60 mV in symmetrical K^+. Open probability increased with voltage, two channels were activated at 40 mV compared to one at −20 mV. (*B*) Records of unitary currents in asymmetrical (140 mM $[K^+]_o$ and 5 mM $[K^+]_i$) solutions at different potentials. Open probability again increased with voltage. (*C*) A summary of the *i-v* relationship in the two conditions described in *A* and *B*. (■) Represents data (mean ± SEM) from 24 patches in symmetrical (140 mM) K^+ solutions. The slope fitted by linear regression was 235 ± 3 pS and reversal occurred at −6 ± 0.4 mV. The $[Ca^{2+}]$ was either 1 or 10 μM. (●) Represents data (mean ± SEM) from 9 patches in asymmetrical K^+ solutions, the curve was fitted with the GHK equation using a P_K value of 4.55×10^{-13} cm^3sec^{-1}. The extrapolated reversal potential was close to E_K and the $[Ca^{2+}]$ was approximately 1 μM. In most cases, the errors bars were located within the symbol for both data sets.

number of channels activated close to this reversal potential. The channel permeability value calculated earlier was used in the constant field (GHK) equation (Goldmann, 1943). The *i-v* relationship in asymmetrical K^+ solutions was well fitted using the value of 4.55×10^{-13} cm^3sec^{-1}. Another typical feature of BK_{Ca} channels is that their open probability is voltage dependent. Examples of unitary current activity in asymmetrical, symmetrical K^+ solutions at different potentials (displaying their voltage-dependence) and the *i-v* relationships under the two different ionic (both symmetrical and asymmetrical K^+ solutions) conditions are shown in Fig. 2*A*, *B* and *C* respectively.

Outside-Out Patches

Outside-out patches obtained from mesenteric artery smooth muscle cells contained (13 out of 14 patches) large unitary currents whose amplitude and activity increased with patch depolarization. At all potentials, the unitary current was outward in direction. Owing to the decreased activity of this large conductance channel at negative patch potentials, only an extrapolated reversal potential was obtained, which was close to E_K (−82 mV). Figure 3*A* and *B* shows examples of these large unitary currents at different patch potentials and the current voltage (*i-v*) relationship respectively. The *i-v* relationship was fitted by the Goldmann, Hodgkin and Katz (GHK) equation using an average permeability value of K^+ (P_K) of 4.55×10^{-13} cm^3sec^{-1}, which was calculated earlier. The activity of the large conductance channels increased with depolarization, such that multiple openings were often observed at large positive patch potentials. The open probability (P_o) was clearly voltage-dependent which is illustrated in Fig. 3*C* and *D*, which shows the channel activity at different patch potentials and the relationship between P_o and voltage, respectively.

Iberiotoxin (50 nM) reversibly inhibited the activity (P_o) of the channels ($n = 3$, $P < 0.05$), although the

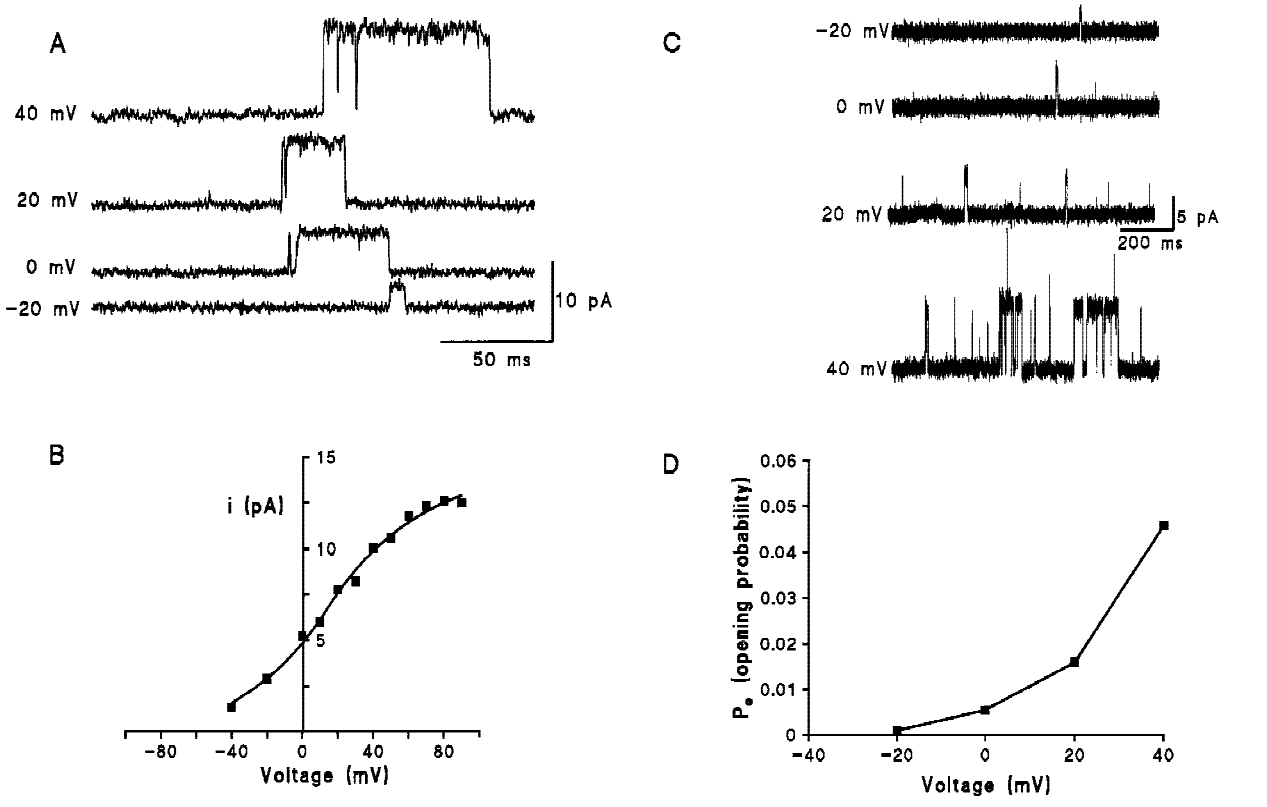

Fig. 3. Large unitary currents present in outside-out patches obtained from freshly dispersed mesenteric smooth muscle cells. (*A*) Examples of large unitary currents at patch potentials of −20, 0, 20 and 40 mV. The unitary current amplitude increased with voltage. (*B*) The *i-v* relationship of the unitary currents shown in *A.* The unitary current amplitude was determined from amplitude histograms fitted with Gaussian functions. The slope conductance at 0 mV was 107 pS. The data were fitted using the Goldmann Hodgkin and Katz (GHK) equation with a P_K value of 4.55×10^{-13} cm^3sec^{-1}. The extrapolated reversal potential was close to E_K (−82 mV). (*C*) Examples of the activity of large unitary currents at different patch potentials. Channel activity increased with voltage. (*D*) Plot of the open probability (P_o) against voltage for the patch shown in (*C*). P_o increased with voltage.

single-channel current amplitude was unaffected ($n = 3$, $P > 0.05$). The channels spent longer periods in the closed state in the presence of iberiotoxin. Apamin (200 nM) had no effect on either P_o or the unitary current amplitude of these channels ($n = 3$, $P > 0.05$). Fig. 4 *A* and *B* shows the effect of iberiotoxin and apamin on BK_{Ca}. The effect of extracellular TEA (1 mM) was different, in that the unitary current amplitude was decreased ($P < 0.05$, $n = 6$), but it appeared to have no effect on the number of channel openings ($P > 0.05$, $n = 6$). Figure 4*C* shows the effect of 1-mM TEA on a large conductance channel in an outside-out patch. In another two outside-out patches, this large conductance channel was also reversibly inhibited by 50 nM charybdotoxin (*data not shown*). The effect of charybdotoxin was very similar to iberiotoxin, in that P_o was decreased (channels showed long closures), but there was no effect on the unitary current amplitude.

Sublevels

Subconductance levels are a common feature of many different ion channels (Fox, 1987). Subconductance levels were also evident in BK_{Ca} channels from rabbit mesenteric arteries, although they were not common (<0.1% of openings). The criteria of Fox (1987) was applied in order to determine the occurrence of subconductance levels: (i) a channel substate should interconvert with the channel mainstate. (ii) the substate should only be observed in the presence of channel mainstate activity. (iii) one must exclude the possibility that the mainstate is the superposition of two independent channels. Two different sublevels around a 1/3 and 1/2 of the mainstate level were seen and these are displayed in Fig. 5. Owing to the rare occurrence of these two sublevels they were not subject to any further analysis.

Effect of $[Ca^{2+}]$ and Voltage on P_o

When patches were stepped from −70 to 70 mV (in 10-mV steps) for 200 msec, in the presence of 0.1 μM Ca^{2+}, channels were observed mainly at large test potentials of 50, 60 and 70 mV. Raising the $[Ca^{2+}]$ lowered the threshold of activation to less positive test potentials (20, 30, 40 mV) and in some cases, activation occurred at

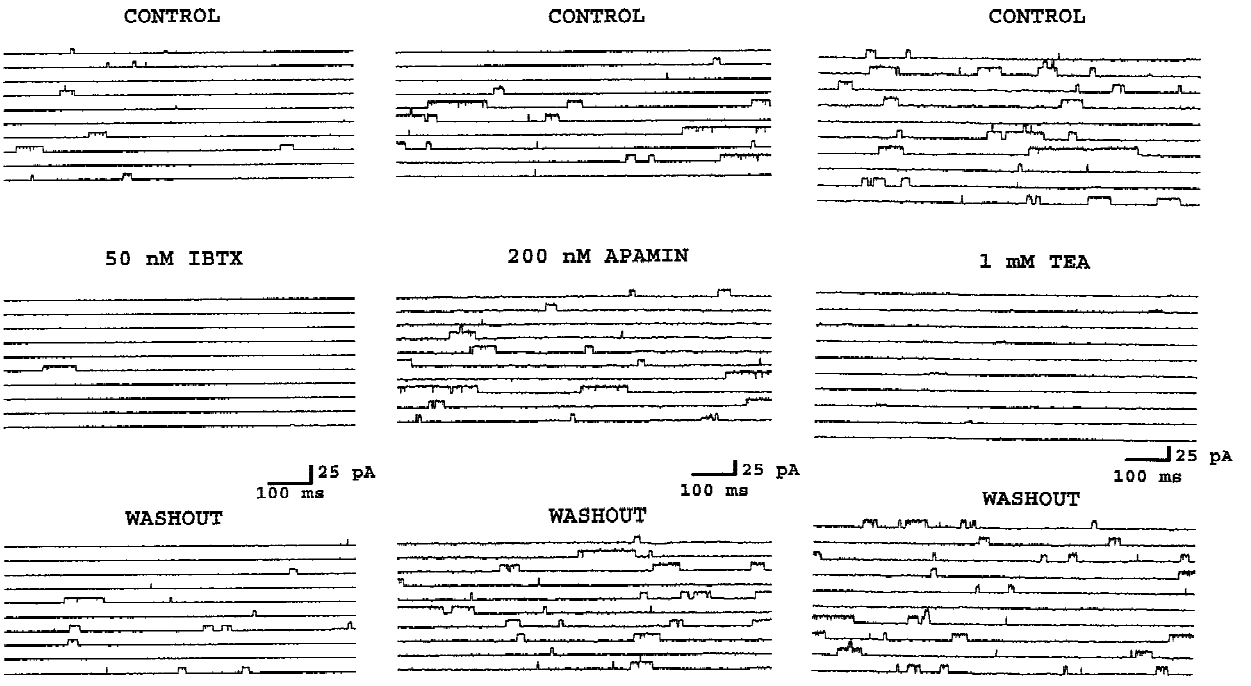

Fig. 4. Effect of extracellular application of iberiotoxin, apamin and TEA on unitary K^+ currents present in outside-out patches. The left hand panel show control traces of activity of large conductance K^+ channels. Unitary current amplitude was 8.88 pA in this case. In the presence of 50 nM iberiotoxin, the open probability of the channel was reduced, but there was no effect on the unitary current amplitude (8.95 pA). The effect of iberiotoxin was reversed upon washout. The open probability was 0.0269 ± 0.0038 in control, compared to 100 nM iberiotoxin, where it was 0.0080 ± 0.0029 ($P \leq 0.05$) and following washout, 0.0330 ± 0.0056. Patch potential was 40 mV. The middle panel illustrates control traces showing activity of K^+ channels. In the presence of 200 nM apamin, the activity of the channel was similar to that observed in control. Channel activity on washout, was also similar to that recorded in control/apamin. The open probability was 0.0882 ± 0.0117 in control conditions, while in 200 nM apamin it was 0.1119 ± 0.0117 and after washout, the open probability was 0.1102 ± 0.0147. The patch potential was 70 mV. The right hand panel shows the effect of TEA (1 mM) on the activity of large conductance K^+ channel in an outside patch. The control traces show activity of large conductance K^+ channels. In the presence of 1 mM TEA, the unitary current amplitude of the channel was significantly reduced (<20% of control) but channel openings still occurred. The effect of TEA was fully reversible upon washout and the patch potential was 70 mV.

negative potentials. Furthermore, with raised $[Ca^{2+}]$, the number of channels activated at 50, 60 and 70 mV was greatly increased. Figure 6*A* demonstrates the effect of raising $[Ca^{2+}]$ on channel activity at test potentials of 70 mV in 0.1, 1.0 and 10.0 μM Ca^{2+}. The average current trace at 70 mV is depicted in these three conditions. Using the averaged current records at 70 mV, the current at the end of a 200-msec step in 1.0 μM Ca^{2+} was 600.8 ± 239% ($n = 6$) greater than in 0.1 μM Ca^{2+}. Similarly, in 10 μM Ca^{2+}, it increased to 672.7 ± 110.0% ($n = 4$) greater than that seen in 0.1 μM Ca^{2+}. The mean current was not fitted with exponentials owing to the large variation in the activation time course of BK_{Ca} channels between different patches, moreover, in some patches, with raised $[Ca^{2+}]$, the mean current was found to increase and then decline (decay) during the 200-msec step. An example of this type of BK_{Ca} activity with $[Ca^{2+}]_i$ is shown in Fig. 6*B*. Slope conductances in 0.1, 1 and 10 μM Ca^{2+} were 235 ± 7.8 pS ($n = 12$), 220 ± 6.6 pS ($n = 7$) and 220 ± 9.1 pS ($n = 4$), respectively ($P > 0.05$, ANOVA) and reversal potentials in 0.1, 1.0 and 10.0 μM Ca^{2+} were −4.3 ± 2 mV ($n = 12$), −4.4 ± 1.8 mV ($n = 7$) and −4.3 ± 1.1 mV ($n = 4$), respectively ($P > 0.05$, ANOVA).

Owing to the variable activity of BK_{Ca} activity with $[Ca^{2+}]_i$ as shown in Fig. 6, the effect of $[Ca^{2+}]$ and voltage on P_o of the BK_{Ca} channel activity was studied in more detail by plotting open probability against voltage and fitting the data with Boltzmann functions. As described earlier, raising $[Ca^{2+}]$ activated BK_{Ca} at less negative potentials and activated additional BK_{Ca} channels present in the patch. Figure 7*A* shows the effect of 0.1 and 1.0 μM Ca^{2+} on an inside-out patch containing 3 BK_{Ca} channels at potentials of −40, 40 and 80 mV in symmetrical K^+ solutions. At −40 mV, with 0.1 μM Ca^{2+}, channel openings were absent and when the $[Ca^{2+}]$ was increased to 1.0 μM Ca^{2+}, two large inward channels were activated. P_o increased with voltage in both $[Ca^{2+}]$. The open probability was plotted against voltage for the patch shown in Fig. 7*A*. Boltzmann functions were fitted to the data points and this is illustrated in Fig. 7*B*. In this patch increasing $[Ca^{2+}]$ shifted the activation curve to the left ($V_{1/2}$ became more negative) and k values were not

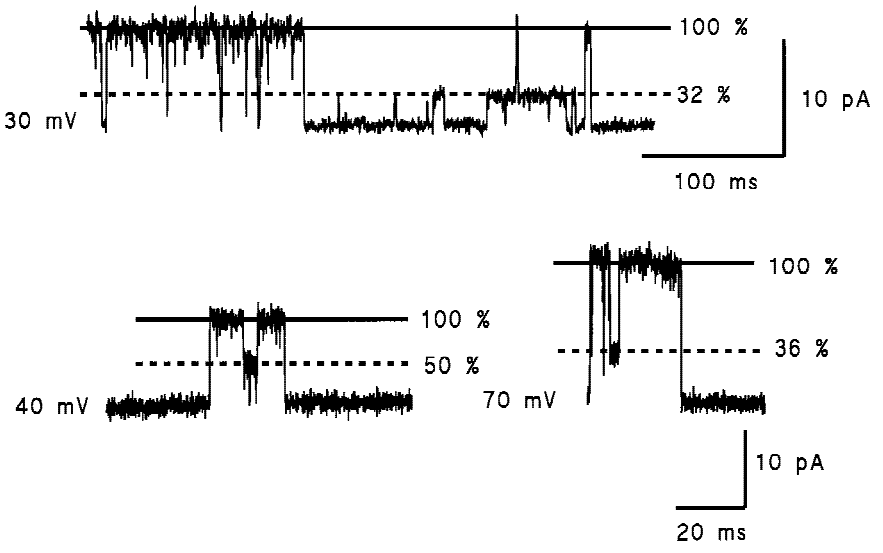

Fig. 5. Subconductance levels of BK_{Ca} channels observed in inside-out patches. The top trace shows a sublevel of 32%, the second trace, a sublevel at 50% and the third trace a sublevel at 36% of the mainstate (100%) level. The bath contained 0.1 μM Ca^{2+} for all three recordings.

affected. It must be stressed that the relationship shown in Fig. 7*B* is somewhat atypical. Most of the plots between P_o and voltage were not as S-shaped and often P_o values approaching 1 was not attainable, even with high (10 μM) Ca^{2+} and large positive voltages. Considerable variability in the values of $V_{1/2}$ and k derived from Boltzmann relationships were found. An example of a somewhat more typical relationship between P_o and voltage is shown in Fig. 8*A*. Raising $[Ca^{2+}]$ shifted the activation curve to the left ($V_{1/2}$ values more negative), but also tended to decrease the slope of the curve (k values became larger). Average values of k were significantly increased in both 1 and 10 μM Ca^{2+} compared to that observed in 0.1 μM Ca^{2+}. The effect of $[Ca^{2+}]$ on k and $V_{1/2}$ from a number of patches is shown graphically in Fig. 8*B* and *C*, respectively. From Fig. 8*C*, the slope calculated by linear regression was 47.9 ± 7.6 mV, hence for a 10-fold increase in $[Ca^{2+}]$ there was nearly a 48-mV shift in $V_{1/2}$. In some cases, inside-out patches were obtained from the same cell, even in these patches, the BK_{Ca} channel showed variability in both $V_{1/2}$ and k. The data were also analyzed on double logarithmic axes i.e., log P_o *vs.* log $[Ca^{2+}]$ (Hill plots; *data not shown*). These plots were fitted with linear relationships with a slope of 1.40 at 40 mV, 1.68 at 20 mV and 1.33 at −20 mV, indicating that approximately two calcium ions must bind to stabilize fully the channel in the open configuration (Barrett, Magleby & Pallota, 1982).

Effect of NS 1619

The BK_{Ca} channel activator NS 1619 (Edwards et al., 1994; Olesen et al., 1994) had a similar effect to increases in $[Ca^{2+}]_i$ in inside-out patches. Channel openings occurred at more negative potentials and an increasing number of channels were activated at positive test potentials with NS 1619. Figure 9 shows the unitary current activity in 0.1 μM Ca and in 0.1 μM Ca with 30 μM NS 1619 at patch potentials of 40–70 mV. The average current trace at 70 mV under the two conditions is shown in the lower portion of the figure. In the presence of NS 1619, the current at the end of the test potential (70 mV) was 427 ± 81.74% ($n = 7$) greater than in control. The slope conductance in the presence and absence of 30 μM NS 1619 was 244 ± 8.9 pS ($n = 8$) and 235 ± 7.7 pS ($n = 12$), respectively ($P > 0.05$). The reversal potentials were −5.3 ± 2.2 mV ($n = 8$) and −4.3 ± 2.0 mV ($n = 12$) ($P > 0.05$), respectively. The effect of 30 μM NS 1619 on P_o of BK_{Ca} channels was also investigated using Boltzmann relationships. From 4 patches, values of $V_{1/2}$ in 0.1 μM Ca^{2+} was 87.0 ± 4.8 mV and with 30 μM NS 1619, it decreased to 48.7 ± 7.9 mV. Values of k were not affected with values being 15.3 ± 1.6 mV and 18.6 ± 3.2 mV in the absence and presence of NS 1619 respectively ($P > 0.05$).

Effect of Intracellular TEA^+

To study the actions of TEA in detail, all experiments were carried out in the presence of 0.1 μM Ca^{2+}, this was to reduce the number of BK_{Ca} channels activated within the patch. 1 mM TEA applied to the intracellular aspect of an inside-out patch had little effect on unitary current amplitude. Increasing [TEA], however, produced a concentration-dependent reduction in the unitary current amplitude (*see* Fig. 10*A* and *B*). The relation between the normalized current amplitude and [TEA] was plotted. Data points were fitted (using least squares method) by the Hill equation, K_d was 58.95 mM and the Hill coefficient was 1.27 (Fig. 10*C*). The reduction in the unitary

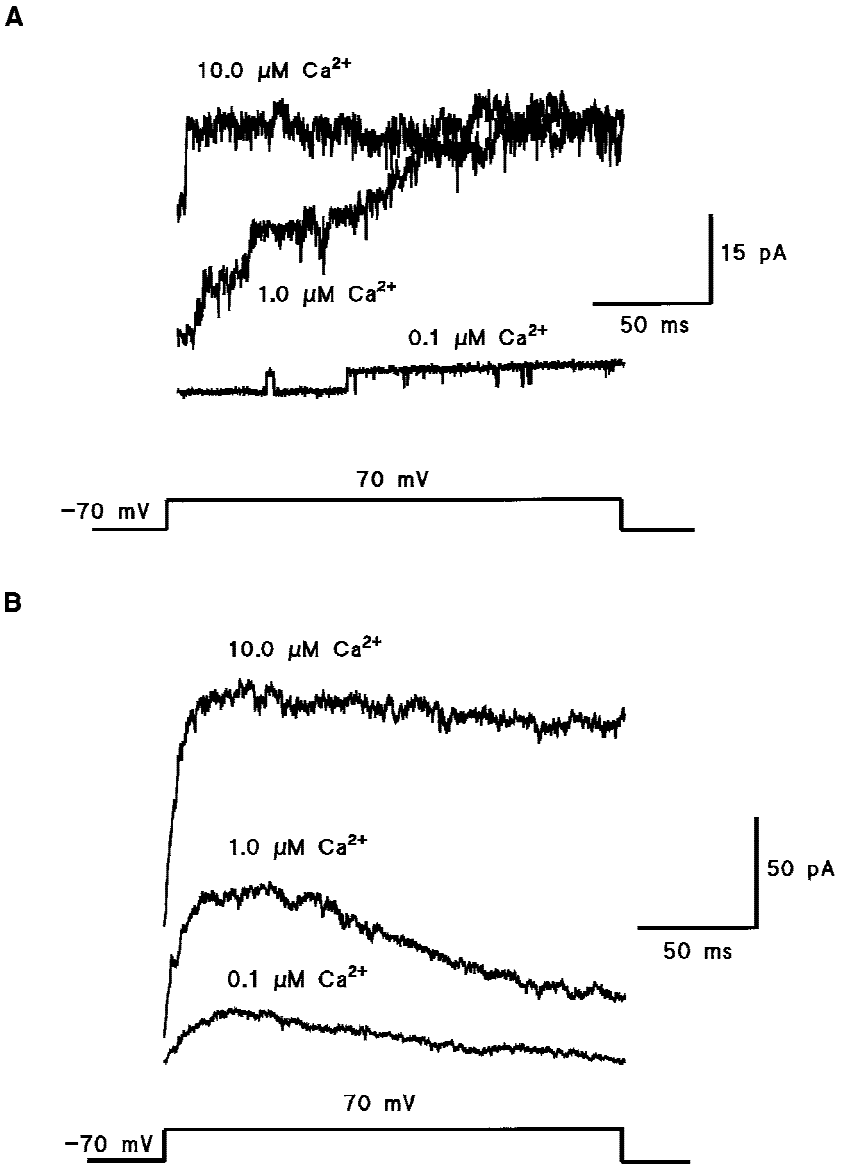

Fig. 6. Examples of different types of BK_{Ca} channel activity in two inside-out patches in 0.1, 1 and 10 μM Ca^{2+}. In both cases, the patch was stepped from −70 to 70 mV for 200 msec. (*A*) In 0.1 μM Ca^{2+}, single individual BK_{Ca} channels can be observed at 70 mV. A maximum of two channels were activated during each step and the average current at 70 mV (from 6 trials) is shown. In 1 μM Ca^{2+}, the activity of the patch was greatly increased, reflecting the activation of several ion channels. The average current (from 6 trials) at 70 mV is shown. The current is larger at the end of the step. In 10 μM Ca^{2+}, the activity of the patch was enhanced, with channels activated earlier in the step compared to either 0.1 or 1 μM Ca^{2+}. The average current (from 6 trials) at 70 mV is shown. (*B*) Examples of BK_{Ca} channel activity in another inside-out patch. The bottom trace shows average current (from 6 trials) in 0.1 μM Ca^{2+}, the current increased and then declined during the duration of the step. The middle trace shows the average current (from 6 trials) in 1.0 μM Ca^{2+}. The current was increased compared to that recorded in 0.1 μM Ca^{2+}. The top trace shows the average (from 6 trials) current in 10.0 μM Ca^{2+}. The decay of the current was less than that seen in either 0.1 or 1.0 μM Ca^{2+}. This patch contained several BK_{Ca} channels.

current amplitude was not detectably voltage-dependent. For example, in one patch with 1 mM TEA, the fractional block of unitary current amplitude at 20, 30, 40, 50, 60, and 70 mV was 0.984, 0.953, 0.959, 0.942, 0.953, and 0.963 respectively. The voltage-dependence of the block was assessed using a modified version of the Woodhull (1973) equation

$$K_d = K_d(0)\exp(-z'VF/RT)$$

in which $K_d(0)$ is the dissociation constant at 0 mV and z′ is the equivalent valence of the blocking reaction, this represents the electrical distance to the TEA binding site from the site of application. Individual values of K_d were obtained. A plot of log K_d against voltage is shown Fig. 10*D*. The line was fitted by the Boltzmann relation $K_d = K_d(0)\exp(-z'VF/RT)$. From this relationship, the slope of the line in Fig. 10*D* equals $-z'F/RT$ giving an equivalent valency of the block of 0.005 and the value of K_d at 0 mV was 60.01 ± 10.95 mM.

Discussion

Single-Channel Properties

Inside-out patches from rabbit mesenteric arteries displayed large unitary currents with a slope conductance around 235 pS in 0.1 μM Ca^{2+}. The open probability of BK_{Ca} channels was voltage-dependent. Either, increasing $[Ca^{2+}]_i$ or the application of the BK_{Ca} channel acti-

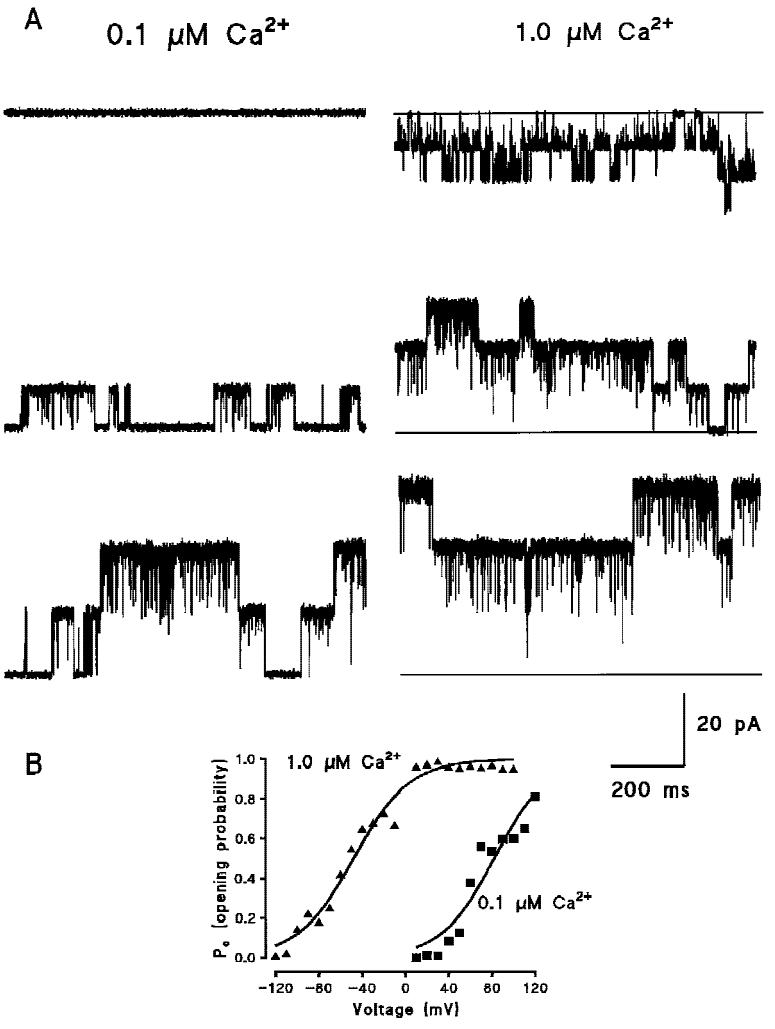

Fig. 7. Voltage and calcium sensitivity of BK_{Ca} channels in inside-out patches. Effect of voltage and $[Ca^{2+}]$ on the open probability (P_o) of K_{Ca} channels. The top, middle and bottom traces show patch activity at −40, 40 and 80 mV, respectively in 0.1 and 1.0 μM Ca^{2+}. At −40 mV in 0.1 μM Ca^{2+}, the patch is quiet, whereas in 1.0 μM Ca^{2+}, two channels are open, the solid line represents the closed level. At 80 mV, in 0.1 μM Ca^{2+}, two channels are activated, whereas in 1.0 μM Ca^{2+}, three channels are active and these channels remained primarily in the open state. The graph shows the relationship between channel activity (P_o), membrane potential and $[Ca^{2+}]$ for the patch shown above. Data were fitted with Boltzmann functions. In 0.1 μM Ca^{2+} (■), $V_{1/2}$ was 81.95 ± 3.77 mV and k was 24.64 ± 3.89 mV. In 1.0 μM Ca^{2+} (▲), $V_{1/2}$ was −48.08 ± 2.25 mV and k was 25.96 ± 2.11 mV.

vator, NS 1619, activated similar large conductance ion channels, with a reversal potential close to that seen in 0.1 μM Ca^{2+}. Applying either NS 1619 or raising $[Ca^{2+}]_i$ activated BK_{Ca} channels at less positive potentials and the channels were activated at an earlier stage in the test pulse, an effect which was particularly evident in 10 μM Ca^{2+}. The slightly negative reversal potential (−6 mV) obtained in the inside-out patches was possibly due to the additional KOH (approx. 35 mM) required to titrate the EGTA to pH 7.3. The decrease in P_o with iberiotoxin appeared to consist primarily of long closures. Similar findings have been reported for BK_{Ca} channels in rat melanotrophs (Kehl & Wong, 1996) and bovine aorta (Giangiacomo, Garcia & McManus, 1992). Overall, the K^+ selectivity, large unitary conductance, voltage-dependence and pharmacological properties indicated the channel was very similar to BK_{Ca} channels described previously in vascular smooth muscle cells (for review, *see* Nelson & Quayle, 1995). In all of the inside-out patches obtained, we found no evidence for the presence of a small conductance, Ca^{2+}-dependent K^+ channel that in any way resembled the apamin-sensitive K^+ channels which have been described previously (Gebremedhin et al., 1996; Marchenko & Sage, 1996; Vogalis & Goyal, 1997). Subconductance levels are a common feature of ion channels, (Fox, 1987). BK_{Ca} channels from chick lens epithelium (Rae et al., 1990) and canine airway smooth muscle (Stockbridge, French & Man, 1991) have been shown to exhibit a variety of substates. BK_{Ca} channels from rabbit mesenteric arteries exhibit subconductance levels very rarely. Nonetheless, in inside-out patches, two clear sublevels were seen around 1/3 and 1/2 of the mainstate level were present. This, however, does not rule out the possibility that the BK_{Ca} channel may exhibit other sublevels than the two described above.

Effect of NS 1619

NS 1619 produced activation of BK_{Ca} channels in inside-out patches from rabbit mesenteric arteries. A simi-

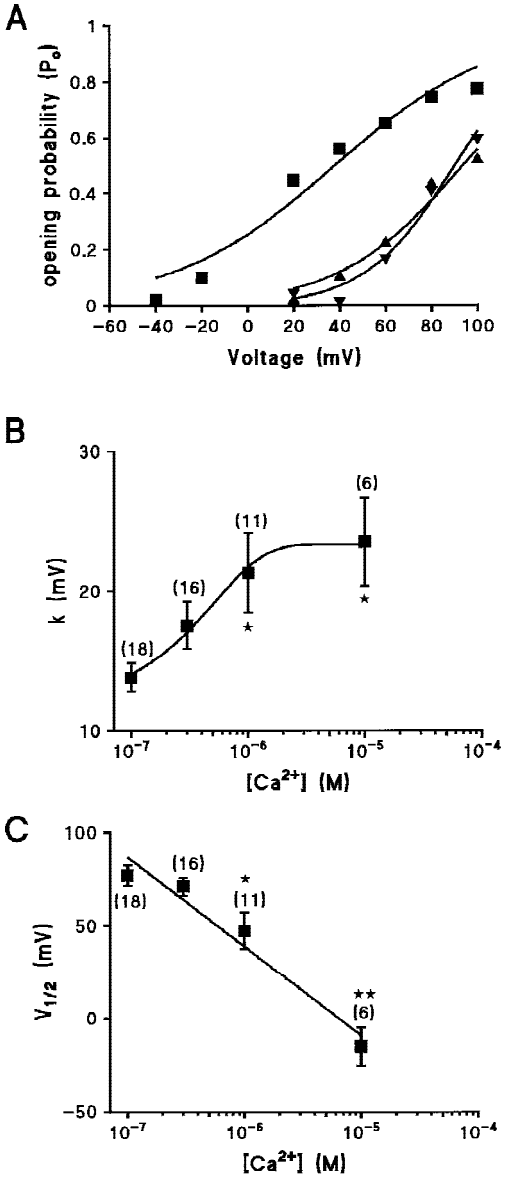

Fig. 8. Variability in k and $V_{1/2}$ of the BK_{Ca} channel with $[Ca^{2+}]_i$. (*A*) A graph showing the relationship between P_o and voltage from an inside-out patch in 0.1, 0.3 and 1.0 μM Ca^{2+}. Increasing $[Ca^{2+}]$ shifted the curve to the left ($V_{1/2}$ more negative) but this also tended to reduce the slope of the curve (k became larger). Data were fitted with Boltzmann relationships. In 1.0 μM Ca^{2+} (■), $V_{1/2}$ was 38.0 ± 5.1 mV and k was 34.9 ± 5.4 mV. With 0.3 μM Ca^{2+} (▲) $V_{1/2}$ was 93.7 ± 3.9 mV and k was 26.9 ± 4.2 mV and in 0.1 μM Ca^{2+} (▼), $V_{1/2}$ was 90.1 ± 2.5 and k was 19.4 ± 2.6 mV. (*B*) From a number of patches, slope factors (k) were obtained from Boltzmann functions and plotted as a function of $[Ca^{2+}]$, k values increased with $[Ca^{2+}]$. Errors bars represent SEM and * indicates $P < 0.05$ compared to values obtained in 0.1 μM Ca^{2+}. The number within the parentheses represent the number of patches. (*C*) The relationship between $V_{1/2}$ and $[Ca^{2+}]$. $V_{1/2}$ was obtained from Boltzmann distributions. A linear function was fitted to the data points and the slope was −47.9 ± 7.6 mV. Error bars represent SEM and significance was compared to values obtained in 0.1 μM Ca^{2+} (*$P <$ 0.05, **$P < 0.001$). The number within the parentheses represent the number of patches.

lar activation of BK_{Ca} has also been described in other tissues (Edwards et al., 1994; Lee, Rowe & Ashford, 1995; MacMillan et al., 1995; Holland et al., 1996). NS 1619 (30 μM) shifted the activation curve to the left ($V_{1/2}$ more negative by 39 mV), but did not affect k. Lee et al., (1995) reached similar conclusions in rat cortical neurones, but along with other workers showed that NS 1619 failed to activate BK_{Ca} in low/zero intracellular calcium solutions (Olesen et al., 1994; Holland et al., 1996). These observations suggest that NS 1619 cannot substitute for Ca^{2+} in activating the channel. It is not clear whether higher concentrations of NS 1619 would produce increases in k values, similar to that seen in high $[Ca^{2+}]$. Our data suggest that NS 1619 produces activation of BK_{Ca} by a direct effect on the channel or a closely associated site, however, the exact mechanism by which this occurs is still not resolved.

Effect of Intracellular TEA

In the present study, we observed that the BK_{Ca} channel was quite resistant to internal TEA (K_d = 59 mM). This value of K_d for TEA is similar to that found by other workers, for example, in growth plate chondrocytes (K_d = 45 mM; Long & Walsh, 1994), in bovine chromaffin cells (K_d = 27 mM, Yellen, 1984), in skeletal muscle t-tubule (K_d = 35 mM, Vergara, 1983), in avian nasal salt gland cells (K_d = 37 mM; Wu, Shuttleworth & Stampe, 1996) and in cultured rat melanotrophs (K_d = 50 mM; Kehl & Wong, 1996). One notable exception, however, is the BK_{Ca} channel from rat cerebral arteries which has a very high (K_d = 0.83 mM) affinity for internal TEA (Wang & Mathers, 1993). The block by TEA represents a fast block. This fast block arises when the mean dwell time of the blocking molecule in the channel pore is less than the response time of the recording system. Hence, the recorded response reflects the time average of the current (Hille, 1992). Davies et al. (1989) showed that block by internal TEA in K_{ATP} channels in skeletal muscle showed two components, both fast and slow. In addition to the fast block which reduced current amplitude (K_d of 26 mM), there was also a fast block which produced brief openings. We found no evidence for a similar slow block in BK_{Ca} channels from rabbit mesenteric arteries. Moreover, this fast block was not detectably voltage-dependent. The value of δ of 0.005 suggests that the block by TEA is at/or close to the mouth of the pore, a similar value to that found for BK_{Ca} channels from cultured rat melanotrophs (Kehl & Wong, 1996). The weak voltage dependence of TEA binding to the internal site reported here and values of the Hill coefficient near 1, indicate that a single TEA molecule moving only a small distance into the electrical field is able to block the BK_{Ca} channel. A simple structural interpretation of these data is that TEA^+ which has the

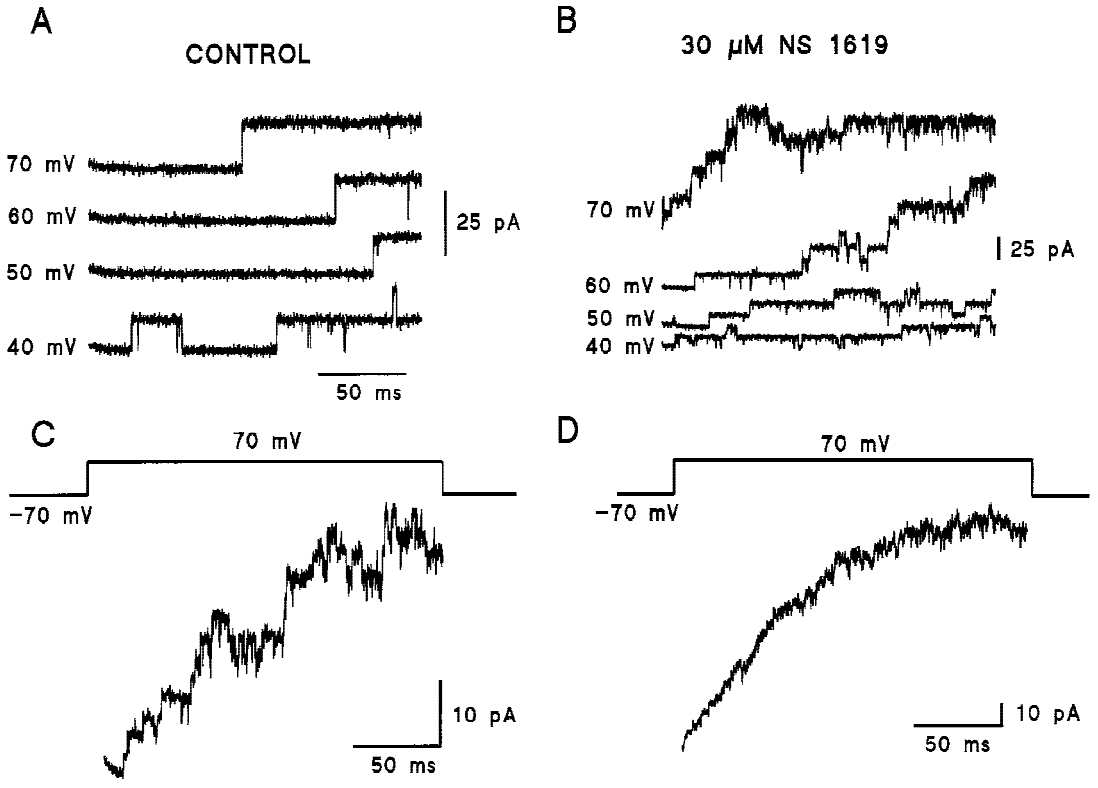

Fig. 9. Stimulatory effect of 30 μM NS 1619 on BK_{Ca} in inside-out patches. (*A*) Examples of BK_{Ca} activity in 0.1 μM Ca^{2+}. The patch was stepped from −70 to 70 mV for 200 msec. Test potentials of 40, 50, 60 and 70 mV are shown for clarity. In 0.1 μM Ca^{2+}, a maximum of two channels were activated during the step to 70 mV. (*B*) Examples of BK_{Ca} activity in 0.1 μM Ca^{2+} and 30 μM NS 1619 (applied to the intracellular face) at test potentials of 40, 50, 60 and 70 mV. With NS 1619, several channels were activated. (*C*) The average current (from 6 trials) at 70 mV in 0.1 μM Ca^{2+}. (*D*) The average current (from 6 trials) at 70 mV in 0.1 μM Ca^{2+} + 30 μM NS 1619.

same radius as hydrated K^+ (0.8 nM) (Latorre & Miller, 1983) enters only part way into the channel before further electrodiffusion is prevented by a narrowing of the pore.

Effect of Calcium on $V_{1/2}$ and K

A couple of surprising aspects of this study was the finding that P_o did not always approach 1 in high [Ca^{2+}] and large positive voltages. Also, the voltage dependence was decreased (increase in *k* values) with high [Ca^{2+}]. Large variation in the mean values of $V_{1/2}$ and *k* were observed. In 0.1, 0.3, 1.0 and 10 μM Ca^{2+}, $V_{1/2}$ was 77.1 ± 5.3, 71.2 ± 4.8, 47.3 ± 10.1 and −14.9 ± 10.1 mV respectively. In bovine mesenteric arteries, Sansom & Stockand (1994) distinguished two BK_{Ca} isochannels, the Ca^{2+} sensitivity of one isochannel being about 50-fold greater than the other. As a result, with 1 μM Ca, the voltages required for half-activation ($V_{1/2}$) were as different as −42 to 47 mV. Highly variable $V_{1/2}$ values have also been described for BK_{Ca} channels from cultured rat melanotrophs (Kehl & Wong, 1996). Reinhart et al., (1991) showed that phosphorylation of the BK_{Ca} channel increased its Ca^{2+} sensitivity and therefore that the Ca^{2+} sensitivity could be underestimated when measured in excised patches compared to cell-attached patches. A similar finding was also suggested for BK_{Ca} channels from pituitary cells (White, Schonbrunn & Armstrong, 1991). Another possibility described recently, is that high (10–1000 μM) [Ca^{2+}] has been shown to induce a low activity mode (i.e., long shut intervals) in BK_{Ca} channels from rat muscle (Rothberg et al., 1996). This may be one explanation for the P_o not reaching 1-in high [Ca^{2+}] in this study (*see also* Sugihara, 1994), along with Ba^{2+} contamination at depolarized voltages from $CaCl_2$ salts (typically about 0.001–0.005% for reagent grade $CaCl_2$) as described by (Neyton & Miller, 1988; Diaz et al., 1995).

BK_{Ca} channels are composed of two dissimilar subunits, α (pore forming) and β (modulatory). Injection of the α subunits alone into *Xenopus* oocytes can produce functional BK_{Ca} channels. However, injection of both α and β subunits, produce BK_{Ca} channels which are more sensitive to both voltage and calcium than BK_{Ca} channels produced by α subunits alone (McManus et al., 1995; Meera et al., 1996). It is plausible that different

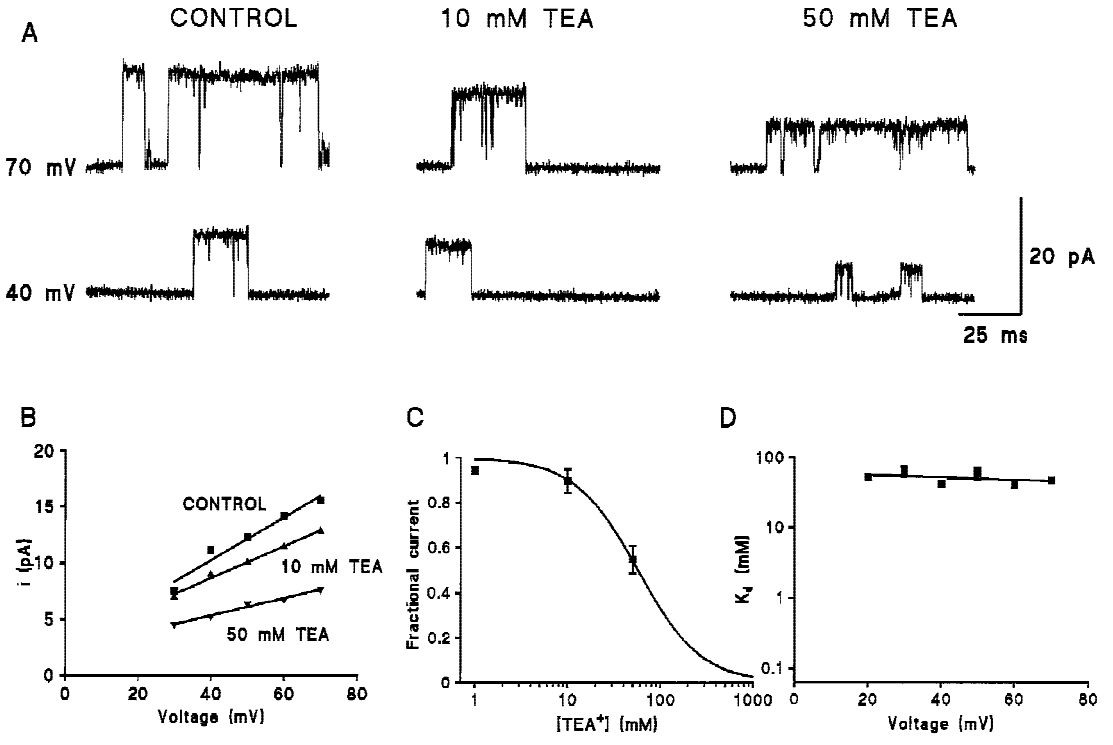

Fig. 10. Effect of internal TEA^+ on BK_{Ca} channels. (*A*) Examples of BK_{Ca} channels at 70 and 40 mV with 10 and 50 mM TEA^+ applied to the intracellular face of an inside-out patch. 10 mM TEA^+ had little effect on current amplitude of K_{Ca} channels, whereas 50 mM TEA^+ reduced the amplitude to less than 50% of control. (*B*) The *i-v* relationship for the patch shown in (*A*). Increasing [TEA^+] reduced the unitary current amplitude of BK_{Ca} channels. (*C*) Concentration dependence of the reduction in single-channel current amplitude by internal TEA^+. The curve was fitted (using least squares) by a Hill equation with a K_d value of 58.95 ± 7.81 mM, and a Hill coefficient (*H*) of 1.26 ± 0.26. The data were obtained at 50 mV. (■) represents data (mean ± SEM) from 4–6 patches. (*D*) Voltage dependence of the block by internal TEA^+. Individual K_d values were obtained and the data were fitted by linear regression. The line was fitted by the Boltzmann relation $K_d = K_d(0)\exp(-z'VF/RT)$, where $K_d(0)$ is the value of K_d at 0 mV, *z* is the equivalent valency of the block, *V* is the membrane potential and *R*, *T*, and *F* have their usual thermodynamic meanings. The equivalent valencies (*z*) of the block was 0.005 and the value of K_d at 0 mV was 60.01 ± 10.95 mM.

proportions or types of subunits may be present in the excised patch, thereby producing BK_{Ca} channels having a variety of sensitivities to both voltage and calcium. If different isoforms of BK_{Ca} are present within the patch, then they could produce relationships between P_o and voltage that are similar to those described here. This notion has recently been corroborated by Tanaka et al. (1997) where most BK_{Ca} channels in excised patches from human coronary smooth muscle are composed of α and β subunits, but channels comprising α subunits alone were seen occasionally. Large variations in $V_{1/2}$ (range −98 to 21 mV) were also recorded suggesting the existence of up to 5 different populations of BK_{Ca}. This variation was attributed to differing coupling of α subunits to the β subunits. This suggestion was also thought to occur for BK_{Ca} channels from avian nasal gland cells to explain their large variation in calcium sensitivity (Wu, Shuttleworth & Stampe, 1996). In the human brain, the β subunit shows a tissue distribution different from that of the α subunit and the idea that the two subunits do not show coupling in certain brain areas has been proposed (Tseng-Crank et al., 1996). Another possible explanation for the variation in $V_{1/2}$ and *k* may be the existence of different splice variants of the channel (Tseng-Crank et al., 1994). The slope of log P_o *vs.* log [Ca^{2+}] (Hill plots) gave mean values around 1.5. This value, however, may be slightly underestimated owing to the observed decrease in P_o found with increasing [Ca^{2+}]. Nonetheless, this suggests that around two molecules of Ca^{2+} are required to stabilize the BK_{Ca} channel in the open configuration. In other tissues, the number of binding sites has been shown to vary, for example, in skeletal muscle values of 2 (Moczydlowski & Latorre, 1983), 3 (Barrett, Magleby & Pallota, 1982) and even 6 (Golowasch, Kirkwood & Miller, 1986). In smooth muscle, values have varied from 3 (Albarwani et al., 1995) to 6 (Carl & Sanders, 1989).

In summary, BK_{Ca} channels from rabbit mesenteric arteries have a number of properties which are similar to those reported in other smooth muscle cells. However, two interesting aspects of BK_{Ca} in this tissue were its weak block (K_d = 59 mM) by internal TEA, perhaps alluding to some structural differences between this channel and that seen in cerebral vascular smooth muscle

(K_d = 0.83 mM). The other finding was that there were large variations in $V_{1/2}$ and k values of BK_{Ca} channels, which suggests that they are capable of displaying a wide range of calcium and voltage sensitivities. Taken together, these results imply that there may be some heterogeneity in BK_{Ca} channels in this vascular tissue. Several different subtypes of K^+ channels have now been described with the recent advance of molecular biology techniques. These methods will in future prove to be invaluable in determining the existence and function of different subtypes (isoforms) of BK_{Ca} channels in the vascular system.

This work was supported by the Wellcome Trust. The authors would also like to thank Drs. Phil Aaronson and Sergey Smirnov for their advice in techniques for dissociating smooth muscle cells.

References

Albarwani, S., Robertson, B.E., Nye, P.C.G., Kozlowski, R.Z. 1994. Biophysical properties of Ca^{2+} and Mg-ATP activated K^+ channels in pulmonary arterial smooth muscle cells isolated from the rat. *Pfluegers Arch.* **428:**446–454

Asano, M., Masuzawalto, K., Matsuda, T., Suzuki, Y., Oyama, H., Shibuya, M.J. 1993. Functional role of charybdotoxin-sensitive K^+ channels in the resting state of cerebral, coronary and mesenteric arteries of the dog. *J. Pharm. Exp. Therap.* **267:**1277–1285

Barrett, J.N., Magleby, K.L., Pallota, B. 1982. Properties of single-calcium activated potassium channels in cultured rat muscle. *J. Physiol.* **331:**3211–3230

Bolotina, V.M., Najibi, S., Palacino, J.J., Pagano, P.J., Cohen, R.A. 1994. Nitric oxide directly activates calcium-dependent potassium channels in vascular smooth muscle. *Nature* **368:**850–852

Brayden, J.E., Nelson, M.T. 1992. Regulation of arterial tone by activation of calcium-dependent potassium channels. *Science* **256:**532–535

Carl, A., Sanders, K.M. 1989. Ca^{2+}-activated K^+ channels in canine colonic myocytes. *Am. J. Physiol.* **257:**C470–C480

Davies, N.W., Spruce, A.E., Standen, N.B., Stanfield, P.R. 1989. Multiple blocking mechanisms of ATP-sensitive potassium channels of frog skeletal muscle by tetraethylammonium ions. *J. Physiol.* **413:**31–49

Diaz, F., Wallner, M., Stefani, E., Toro, L., Latorre, R. 1995. Barium blockade of a clone Ca^{2+}-activated K^+ channel (*hslo*) expressed in *Xenopus laevis* oocytes. *Biophysical Journal* A29 (*Abstr.*)

Edwards, G., Neiderste-Hollenberg, A., Schneider, J., Noack, T.H., Weston, A.H. 1994. Ion channel modulation by NS 1619, the putative BK_{Ca} channel opener, in vascular smooth muscle. *Br. J. Pharmacol.* **113:**1538–1547

Fox, J.A. 1987. Ion channel subconductance states. *J. Membrane Biol.* **97:**1–9

Gebremedhin, D., Kaldunski, M., Jacobs, E.R., Harder, D.R., Roman, R.J. 1996. Coexistence of two types of Ca^{2+}-activated K^+ channels in rat renal arterioles. *Am. J. Physiol.* **270:**F69–F81

George, M.J., Shibata, M.F. 1995. Regulation of calcium-activated potassium channels by S-nitrosothiol compounds and cyclic guanosine monophosphate in rabbit coronary myocytes. *J. Invest. Medicine* **43:**451–458

Giangiacomo, K.M., Garcia, M.L., Mcmanus, O.B. 1992. Mechanism of iberiotoxin block of the large conductance calcium-activated potassium channel from bovine aortic smooth muscle. *Biochemistry* **31:**6719–6727

Goldmann, D.E. 1943. Potential impedence and rectification in membranes. *J. Gen. Physiol.* **27:**37–60

Golowasch, J., Kirkwood, A., Miller, C. 1986. Allosteric effects of Mg^{2+} on the gating of Ca^{2+}-activated K^+ channels from mammalian skeletal muscle. *J. Exp. Biol.* **124:**5–13

Hamill, O.P., Marty, A., Neher, E., Sakmann, B., Sigworth, F.J. 1981. Improved patch-clamp technique for high resolution current recording from cells and cell-free membrane patches. *Pfluegers Arch.* **39:**85–100

Hille, B. 1992. Ionic channels of excitable membranes, 2nd edition Sinauer Associates. Sunderland, MA

Holland, M., Langton, P.D., Standen, N.B., Boyle, J.P. 1996. Effects of the BK_{Ca} channel activator, NS 1619, on rat cerebral artery smooth muscle. *Br. J. Pharmacol.* **117:**119–129

Kehl, S.J., Wong, K. 1996. Large conductance calcium-activated potassium channels of cultured rat melanotrophs. *J. Membrane Biol.* **150:**219–230

Lee, K., Rowe, I.C.M., Ashford, M.L.J. 1995. NS 1619 activates BK_{Ca} channel activity in rat cortical neurones. *Eur. J. Pharmacol.* **280:**215–219

Lattorre, R., Miller, C. 1983. Conduction and selectivity in potassium channels. *J. Membrane Biol.* **71:**11–30

Long, K.J., Walsh, K.B. 1994. A calcium-activated potassium channel in growth plate chondrocytes: regulation by protein kinase A. *Biochem. Biophys. Res. Comm.* **201:**776–781

MacMillan, S., Sheridan, R.D., Chilvers, E.R., Patmore, L. 1995. A comparison of the effects of SA40, NS 004 and NS 1619 on large conductance Ca^{2+}-activated K^+ channels in bovine tracheal smooth muscle cells in culture. *Br. J. Pharmacol.* **16:**1656–1660

Marchenko, S.M., Sage, S.O. 1996. Calcium-activated potassium channels in the endothelium of intact rat aorta. *J. Physiol.* **492.1:**53–60

Meera, P., Wallner, M., Jiang, Z., Toro, L. 1996. A calcium switch for the functional coupling between α (hslo) and β subunits ($K_{V,Ca\beta}$) of maxi K channels. *FEBS Lett.* **382:**84–88

McManus, O.B., Helms, L.M.H., Pallanck, L., Ganetzky, B., Swanson, R., Leonard, R.J. 1995. Functional role of the β subunit of high conductance calcium-activated potassium channels. *Neuron* **14:**645–650

Moczydlowski, E., Latorre, R. 1983. Gating kinetics of Ca^{2+}-activated K^+ channels from rat muscle incorporated into planar bilayers. *J. Gen. Physiol.* **82:**511–542

Mistry, D.K., Garland, C.J. 1996. Large conductance Ca^{2+}-activated K^+ channels but not apamin-sensitive K^+ channels in smooth muscle cells isolated from the rabbit mesenteric artery. *Br. J. Pharmacol.* **119:**167*P*

Nelson, M.T., Quayle, J.M. 1995. Physiological roles and properties of potassium channels in arterial smooth muscle. *Am. J. Physiol.* **268:**C799–C822

Neyton, J., Miller, C. 1988. Potassium blocks barium permeation through a calcium-activated potassium channel. *J. Gen. Physiol.* **92:**549–567

Olesen, S-P., Munch, E., Moldt, P., Drejer, J. 1994. Selective activation of Ca^{2+}–dependent K^+ channels by novel benzimadazolone. *Eur. J. Pharmacol.* **251:**53–59

Rae, J.L., Dewey, J., Rae, J.S., Cooper, K. 1990. A maxi calcium-activated potassium channel from chick lens epithelium. *Curr. Eye Res.* **9:**847–861

Reinhart, P.H., Chung, S., Martin, B.L., Brautigan, D., Levitan, I.B. 1991. Modulation of calcium-activated potassium channels from rat brain by protein kinase A and phosphatase 2A. *J. Neurosci.* **11:**1627–1635

Rothberg, B.S., Bello, R.A., Song, L., Magleby, K.L. 1996. High Ca^{2+} concentrations induce a low activity mode and reveal Ca^{2+}-

independent long shut intervals in BK channels from rat muscle. *J. Physiol.* **493.3:**673–689

Sansom, S.C., Stockand, J.D. 1994. Differential Ca^{2+} sensitivities of BK(Ca) isochannels in bovine mesenteric vascular smooth muscle. *Am. J. Physiol.* **266:**C1182–C1189

Stockbridge, L.L., French, A.S., Man, S.F.P. 1991. Subconductance states in calcium-activated potassium channels from canine airway smooth muscle. *Biochem. Biophys. Acta* **1064:**221–218

Sugihari, I. 1994. Calcium-activated potassium channels in goldfish hair cells. *J. Physiol.* **476:**373–390

Tanaka, Y., Meera, P., Song, M., Knaus, H-G., Toro, L. 1997. Molecular constituents of maxi KCa channels in human coronary smooth muscle: predominant α and β subunit complexes. *J. Physiol.* **502.3:**545–559

Trieschmann, U., Isenberg, G. 1989. Ca^{2+}-activated K^+ channels contribute to the resting potential of vascular myocytes. Ca^{2+}-sensitivity is increased by intracellular Mg^{2+} ions. *Pfluegers Arch.* **414:**S183–S184

Tseng-Crank, J., Foster, C.D., Krause, J.D., Mertz, R., Godinot, N., Dichiara, T.J., Reinhart, P.H. 1994. Cloning, expression and distribution of functionally distinct Ca^{2+}-activated K^+ channel isoforms from human brain. *Neuron* **13:**1315–1330

Tseng-Crank, J., Godinot, N., Johansen, T.E., Ahring, P.K., Strobaek, D., Mertz, R., Foster, C.D., Olesen, S.P., Reinhart, P.H. 1996. Cloning, expression and distribution of a Ca^{2+}-activated K^+ channel beta subunit from human brain. *Proc. Natl. Acad. Sci. USA* **93:**9200–9205

Vergara, C. 1983. Characterization of a Ca^{2+}-activated K^+ channel from skeletal muscle membranes in artificial bilayers. PhD Dissertation, Harvard University Cambridge, MA

Vogalis, F., Goyal, R.K. 1997. Activation of small conductance Ca^{2+}-dependent K^+ channels by purinergic agonists in smooth muscle cells of the mouse ileum. *J. Physiol.* **502.3:**497–509

Wang, Y., Mathers, D.A. 1993. Ca^{2+}-dependent K^+ channels of high conductance in smooth muscle cells isolated from rat cerebral arteries. *J. Physiol.* **462:**529–545

White, R.E., Schonbrunn, A., Armstrong, D.L. 1991. Somatostatin stimulates Ca^{2+}-activated potassium channels through protein dephosphorylation. *Nature* **351:**570–573

Woodhull, A.M. 1973. Ionic blockade of sodium channels in nerve. *J. Gen. Physiol.* **84:**157–186

Wu, J.V., Shuttleworth, T.J., Stampe, P. 1996. Clustered distribution of calcium sensitivities: An indication of hetero-tetrameric gating components in Ca^{2+}-activated K^+ channels reconstituted from avian nasal gland cells. *J. Membrane Biol.* **154:**275–282

Yellen, G. 1984. Ionic permeation and blockade in Ca^{2+}-activated K^+ channels of bovine chromaffin cells. *J. Gen. Physiol.* **84:**157–186